Drought Recurrence in the Great Plains as Reconstructed from Long-Term Tree-Ring Records

CHARLES W. STOCKTON AND DAVID M. MEKO

Laboratory of Tree-Ring Research, University of Arizona, Tucson 85721

(Manuscript received 17 May 1982, in final form 19 July 1982)

ABSTRACT

Recently collected tree-ring data were used to reconstruct drought from 1700 to the present in four regions flanking the Great Plains. Regions were centered in Iowa, Oklahoma, eastern Montana and eastern Wyoming. Reconstructions derived by multiple linear regression explained from 44 to 56% of the variance in regionally averaged annual precipitation from 1933 to 1977. Years of widespread severe drought clustered into drought epochs lasting 5–10 years. A weighted mean of the four regional reconstructions pointed out the severity of the 1930's drought; the years 1934, 1936 and 1939 ranked among the driest 10 of 278 years. When drought conditions were averaged over periods of three or more years, the 1930's drought was equaled or surpassed in severity by droughts in the 1750's, 1820's and 1860's. Spectral analysis of the 1700–1977 reconstruction indicated that precipitation averaged over the four regions had a periodicity of 16–19 years, but reconstructions for the individual regions deviated considerably from this result. The Iowa region was dominated by a 22-year periodicity, the Oklahoma region by a 17–23 year periodicity, and the other two regions by a relatively strong 60-year periodicity. Separate analysis of 88-year subperiods of reconstructions indicated that evidence for a 22-year periodicity was strongest in the most recent period (1890–1977), weaker for 1802–89 and lacking entirely from 1714 to 1801.

1. Introduction

Widespread drought in the Great Plains has disrupted farming and caused economic hardship several times in the last 100 years, most notably in the 1890's, 1930's and 1950's. The empirical probability of recurrence of severe drought is of interest to long range planning for agriculture and water resources, but gaged rainfall records cannot depict large scale drought history in the Great Plains back beyond the late 1800's. Recent studies have demonstrated the usefulness of tree rings for extending regional drought history (Cook and Jacoby, 1979; Meko *et al.*, 1980; Duvick and Blasing, 1981; Puckett, 1981). These studies focused on drought conditions in particular states, and were of relatively small geographical extent. On a larger scale, Stockton and Meko (1975) reconstructed spatial patterns of drought over the United States west of the Mississippi River from a grid of tree ring sites scattered over the western United States. Subsequent analysis of that reconstruction indicated that area in drought expanded and contracted rhythmically with a period of 22 years (Mitchell *et al.*, 1979). The results for the Great Plains were tenuous, however, because none of the tree ring sites were located in the Great Plains; the reconstruction model relied on teleconnections between drought in the Great Plains and tree growth in distant mountain ranges.

We have attempted to overcome earlier limitations by collecting new tree ring sites from the western fringe of the Great Plains in the summers of 1980 and 1981. These new data, augmented by Great Plains tree-ring data provided by others, were used in the present study to reconstruct Great Plains drought back to 1700. The objectives were to place the 1930's and 1950's droughts in long-term perspective and to search for evidence of a 22-year periodicity in drought.

2. Data

Tree-ring sites were grouped into the four regions shown in Fig. 1. Descriptive information on the sites is listed in Table 1 and collectors and sponsoring institutions are listed below.

Region	Institution	Collectors
A	Oak Ridge National Laboratory	D. Duvick
B	University of Arkansas	D. Stahle
C, D	University of Arizona	T. Harlan and D. Meko

Although some series extended back earlier than the year 1600, sample depth was adequate for large-scale analyses only for the period 1700 to the present.

Tree-ring data were in the form of indices, annual ring widths standardized to remove the effects of tree age on mean ring width. Standardization consists of

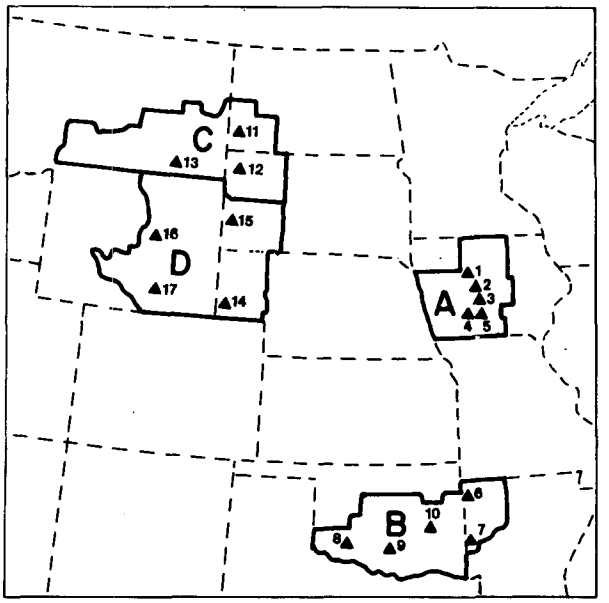

FIG. 1. Map showing regions and tree-ring sites. Regions are designated A, B, C and D; boundaries coincide with outer boundaries of enclosed climatic divisions. Tree-ring sites are marked by triangles, and numbered as in Table 1.

fitting a mathematical function to a ring-width series, and dividing each year's measured ring width by the corresponding value of the function. The procedure amounts to a removal of trend, and necessarily limits information obtainable on long-term climatic trend. The appropriate mathematical function for trend removal varies depending on site environment. Ring width in arid-site conifers often follows a simple decreasing exponential curve, reflecting the gradual increase in tree diameter over time. Ring-width series from more mesic or forest interior sites, on the other hand, may contain transient trends and long-wavelength fluctuations due to stand-density changes or other factors related to changing competition for moisture or light (Fritts, 1976). A more flexible curve may be required for trend removal at such sites. Two functions frequently used are low-order polynomials (Fritts, 1976), and cubic splines (Cook and Peters, 1981). Series from Region A in this study were standardized with cubic splines, series from C and D with decreasing exponentials, and series from B with either polynomials or exponential curves.

Climatic data consisted of station and divisional monthly precipitation and temperature records. Long-term records for selected stations in the four regions were obtained from the files of the University of Arizona Tree-Ring Laboratory. Divisional data for the period 1931–78 were obtained from the National Climate Center in Asheville, N.C. Regional series were computed by averaging divisional data. Regions A, B, C and D encompassed 5, 7, 3 and 5 climatic divisions respectively.

The climatic regions were largely dictated by the natural clustering of tree-ring sites. Mean annual precipitation ranges from less than 16 inches in Regions C and D to more than 40 inches in Region B. The seasonal distribution of precipitation peaks in May and June in all regions.

3. Tree-ring indices as a measure of drought

Tree-ring indices reflect the combined influence of many climatic and biological variables over an in-

TABLE 1. Listing of tree-ring sites.

Site[a] Number	Region	Name	State	Species[b]	Elevation (m)	Sample depth[c] 1900	1800	1700	1600
1	A	Woodman	IA	WO	335	64	49	2	0
2	A	Ledges	IA	WO	320	96	61	14	0
3	A	Back Woods	IA	WO	275	99	41	10	0
4	A	Pammel	IA	WO	305	93	72	17	0
5	A	Ahquabi	IA	WO	305	54	38	3	3
6	B	Wedington	AR	PO	435	46	32	0	0
7	B	Black Fork	AR	WO	700	41	35	2	0
8	B	Quanah	OK	PO	425	47	41	1	0
9	B	Arbuckles	OK	PO	280	28	23	1	0
10	B	Eufaula	OK	PO	215	44	24	0	0
11	C	Burning Coal	ND	PP	790	20	18	8	1
12	C	Slim Butte	SD	PP	1065	34	32	9	0
13	C	Otter Creek	MT	PP	1220	38	34	7	0
14	D	Pumpkin	NE	PP	1465	12	10	4	0
15	D	Custer	SD	PP	1800	38	35	14	1
16	D	Teapot	WY	PP	1615	30	30	12	2
17	D	Rock River	WY	PP	2165	26	24	13	8

[a] Corresponds to numbers on map in Fig.1.
[b] WO White Oak, *Quercus alba* L; PO Post Oak, *Quercus stellata* Wangenh; PP Ponderosa Pine, *Pinus ponderosa* Laws.
[c] Number of cores dating back to the specified year.

definite number of months preceding the end of formation of the annual ring. Various studies have shown that, in spite of the complexity of the system, many tree-ring index series are significantly correlated with meteorological measures of drought such as annual or seasonal precipitation (Schulman, 1956; Fritts, 1962).

Partial correlation coefficients (Panofsky and Brier, 1968) between tree-ring indices used in this study and various monthly groupings of divisional precipitation and mean temperature are summarized in Fig. 2. Each tree-ring index series was correlated with the climatic data from the division containing the tree-ring site for the period 1933–77. A first-order partial correlation coefficient between tree-ring index X_t and divisional precipitation or temperature Y_t was computed, with the influence of "past growth", X_{t-1}, eliminated. A second-order coefficient was also computed between X_t and temperature with influence of both past growth and precipitation eliminated; the intent here was to adjust for intercorrelation between precipitation and temperature.

Of the monthly groupings of climatic data, September through August total precipitation correlated highest with tree-ring indices. Correlation dropped off for shorter monthly groupings. Temperature was of negligible importance in the annual (September–August) grouping: the median partial r was only 0.08 between tree-ring indices and annual mean temperature when influences of both precipitation and past growth were eliminated. In contrast, summer (July–August) temperature was correlated as highly as summer precipitation with tree-ring indices, probably because potential evapotranspiration (PE) is increasingly important to the water balance of trees in summer months.

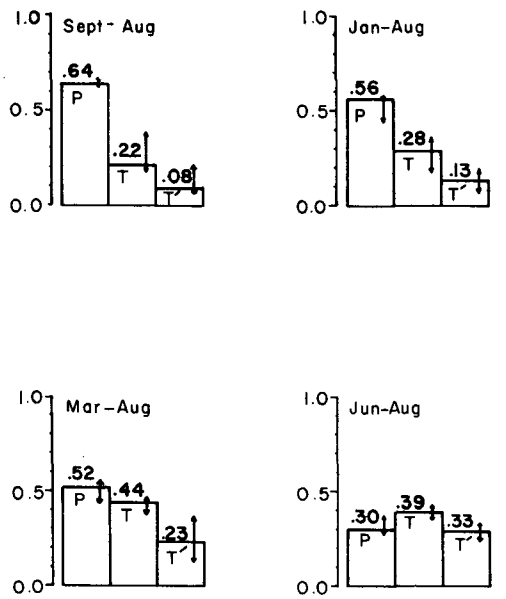

FIG. 2. Partial correlation coefficients of tree-ring indices with divisional precipitation and temperature. Median correlation coefficient for the 17 tree-ring sites is given by height of bar; range within which nine of the 17 correlations fall is given by arrows. Leftmost bar in each group shows partial correlation between tree-ring index and precipitation with effect of past growth (previous years' tree-ring index) eliminated. Middle bar shows corresponding partial correlation of tree-ring index with temperature. Rightmost bar shows partial of tree-ring index with temperature when effects of both past growth and precipitation are eliminated.

4. Reconstruction

a. Method

Tree-ring indices were calibrated with 1933–77 annual (September–August) precipitation by multiple linear regression in two stages: the first to emphasize the local precipitation signal in the individual tree-ring series, and the second to weight the local precipitation signals into estimates of regional precipitation. The regression model for the first phase had as predictand divisional precipitation Y_t in year t, and as predictors tree-ring indices for the current year X_t, and lagged forward, X_{t+1}, and backwards, X_{t-1}. The model is given by:

$$Y_t = a_0 + a_1X_{t-1} + a_2X_t + a_3X_{t+1} + e_t, \qquad (1)$$

where a_0 is a regression constant; a_1, a_2 and a_3 are regression coefficients; and e_t is the residual error.

Coefficients in (1) were estimated by stepwise regression (Draper and Smith, 1966) to get the prediction equation

$$\hat{Y}_t = \hat{a}_0 + \hat{a}_1X_{t-1} + \hat{a}_2X_t + \hat{a}_3X_{t+1}, \qquad (2)$$

where the caret denotes estimated value. Eq. (2) is equivalent to a time filter of the tree-ring index; this is an attempt to compensate for the trees' distributing the effect of a single year's climate anomaly over several rings (Stockton, 1975).

Regression equations for each of the 17 tree-ring sites are listed in Table 2, along with the proportion of variance explained by regression

$$R^2 = [\sum_{t=1}^{N} (\hat{Y}_t - \bar{Y})^2]/\sum_{t=1}^{N} (Y_t - \bar{Y})^2, \qquad (3)$$

where N is the sample size (45 years) and $\bar{Y}$ is the sample mean of Y_t for 1933–77. R^2 is a measure of the strength of the local or divisional precipitation signal in each tree-ring series. Also in Table 2 are values of R^2 adjusted for loss of degrees of freedom

$$R_a^2 = R^2 - \frac{(k-1)}{N-k}(1 - R^2), \qquad (4)$$

where k is the number of predictors and N and R^2 are defined as before. Although the signal in some series was very weak, sites with strong signals were found in all four regions. Unadjusted percent vari-

TABLE 2. Summary of single-site regression equations.

Region	Site	Division	Constant	Coefficients $t-1$	Coefficients t	Coefficients $t+1$	R^2	Adjusted R^2
A	Woodman	1305	5.48		26.44		0.44	0.42
	Ledges	1305	3.45		21.33	7.23	0.44	0.41
	Back Woods	1305	11.86		20.33		0.40	0.39
	Pammel	1308	11.05		22.32		0.31	0.29
	Ahquabi	1308	7.81		25.67		0.41	0.40
B	Wedington	0301	37.78	−25.11	32.51		0.15	0.09
	Black Fork	0304	39.52	−20.06	29.04		0.15	0.11
	Quanah	3407	10.54		17.50		0.46	0.44
	Arbuckles	3408	5.52	−7.33	39.19		0.54	0.52
	Eufaula	3406	7.15	−8.80	44.41		0.41	0.38
C	Burning Coal	3207	12.99	−2.55	5.74		0.44	0.41
	Slim Butte	3901	10.28	−3.21	6.70	1.76	0.49	0.45
	Otter Creek	2407	8.43	−2.62	6.45	1.71	0.41	0.37
D	Pumpkin	2501	16.35	−2.12	2.46		0.13	0.09
	Custer	3904	12.50	−3.11	8.72	2.18	0.45	0.41
	Teapot	WY3[a]	9.92		4.43		0.35	0.33
	Rock River	WY2[b]	10.49	−3.61	5.95		0.46	0.43

[a] Mean of divisions 4805, 4807 and 4808.
[b] Mean of divisions 4808 and 4810.

ance explained by the best series in each region ranged from 44 to 54%. Note that most of the regression equations in Table 2 are simpler than the general $t-1$, t, $t+1$ model of (2): the number of predictors was selected to maximize adjusted R^2 as given by (4).

Long-term indices were substituted into the regression equations to obtain reconstructions of divisional precipitation. These series are referred to here as single-site reconstructions.

The second stage in reconstruction was to weight the single-site reconstruction to obtain least-squares estimates of regional precipitation. Regional precipitation Z_t for 1933–77 was regressed against single-site reconstructions in a region using the following model:

$$Z_t = b_0 + b_1\hat{Y}_{1,t} + b_2\hat{Y}_{2,t} + \cdots + b_m\hat{Y}_{m,t} + e_t, \quad (5)$$

where $\hat{Y}_{i,t}$ is the single-site reconstruction from (2) for the ith site, b_0 is a regression constant, b_1, b_2, . . . , b_m are regression coefficients; and e_t is residual

TABLE 3. Summary of regional regression equations.

Region	Step	Site	Number[a]	Standardized coefficient	R^2	Adjusted[b] R^2
A	1	Ahquabi	5	0.24	0.43	0.41
	2	Ledges	2	0.36	0.47	0.45
	3	Pammel	4	0.14	0.48	0.44
B[c]	1	Arbuckles	9	0.45	0.41	0.40
	2	Eufaula	10	0.38	0.53	0.50
	3	Black Fork	7	0.03	0.53	0.49
B'[c]	1	Arbuckles	9	0.52	0.41	0.40
	2	Black Fork	7	0.15	0.43	0.41
	3	Quanah	8	0.09	0.44	0.40
C	1	Otter Creek	13	0.34	0.41	0.40
	2	Burning Coal	11	0.27	0.52	0.49
	3	Slim Butte	12	0.27	0.55	0.52
D	1	Custer	15	0.41	0.36	0.35
	2	Teapot	16	0.40	0.51	0.49
	3	Pumpkin	14	0.24	0.56	0.54

[a] As in Fig. 1.
[b] For loss of degrees of freedom.
[c] Series B extends only to year 1746; series B' to 1697.

error. Predictors were entered stepwise until R^2 leveled off, with an additional requirement that the final equation contain at least three predictors. Estimation of coefficients yielded the reconstruction equation

$$\hat{Z}_t = \hat{b}_0 + \hat{b}_1\hat{Y}_{1,t} + \hat{b}_2\hat{Y}_{2,t} + \cdots + \hat{b}_m\hat{Y}_{m,t}, \quad (6)$$

where the caret denotes an estimated value.

Regional regression equations are summarized in Table 3. The relative importance of the various tree-ring sites to the regional reconstructions is given by the relative sizes of regression coefficients in (6). These coefficients partly depend on the variance of the predictors; to facilitate comparison, coefficients are given in Table 3 in standardized form:

$$\hat{b}'_i = \frac{S_y}{S_z}\hat{b}_i,$$

where $\hat{b}_i$ is the regression coefficient on the ith predictor from (6), $\hat{b}'_i$ is the corresponding standardized coefficient, and S_z and S_y are, respectively, the sample standard deviations of regional precipitation Z_t and of the single-site reconstruction $\hat{Y}_{i,t}$ for the ith site. The small change in R^2 and small coefficients on the third predictor to enter indicate that the third site contributed little to reconstruction accuracy in Regions A and B.

Single-site reconstructions of divisional precipitation were substituted into the regional regression equations to generate long-term reconstructions of regional precipitation.

b. Accuracy of regional reconstructions

Time series plots (Fig. 3) show that reconstructed regional precipitation agreed well with actual, especially in broad swings above or below the mean. Proportions of variance explained in the 1933–77 calibration period ranged from 0.44 to 0.56. When reconstructions are converted to percent of 1933–77 normal, standard error of reconstruction ranged from 10% in Region D to 13% in Region B. Separate analysis of the 10 wettest and 10 driest years indicated that standard error was up to 3% higher in wet years than in dry, probably because of decreasing sensitivity of tree growth to precipitation above some optimum amount.

Reconstructions were independently verified with precipitation series from selected stations for years before the calibration period. Pairs of series and corresponding correlation coefficients are shown in Fig. 4. Dropoff in correlation from the calibration period to the earlier years would have been taken as evidence of poor verification. In none of the regions did correlation coefficients drop off by more than 0.04, lending support to the calibration period R^2 as a measure of long-term accuracy.

Changing sample size can make calibration-period statistics misleading as measures of accuracy of long-term reconstructions. For example, the Arbuckles, Oklahoma site comprised 28 cores in 1900 and 1 core in 1700 (Table 1). The nonclimatic noise in the tree-

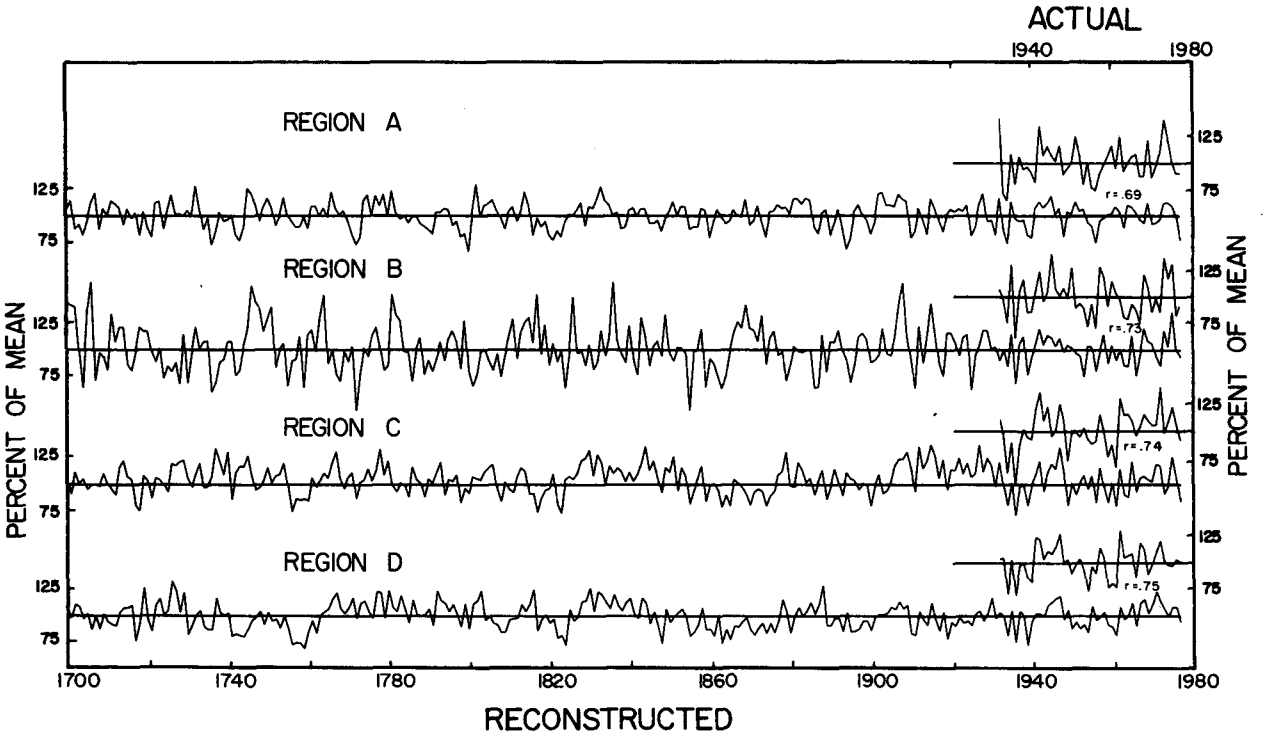

FIG. 3. Time series plots of actual and reconstructed regional precipitation. Series are plotted as percent of 1933–77 normal. Correlation coefficients (r) between actual and reconstructed regional series (1933–77) are also shown.

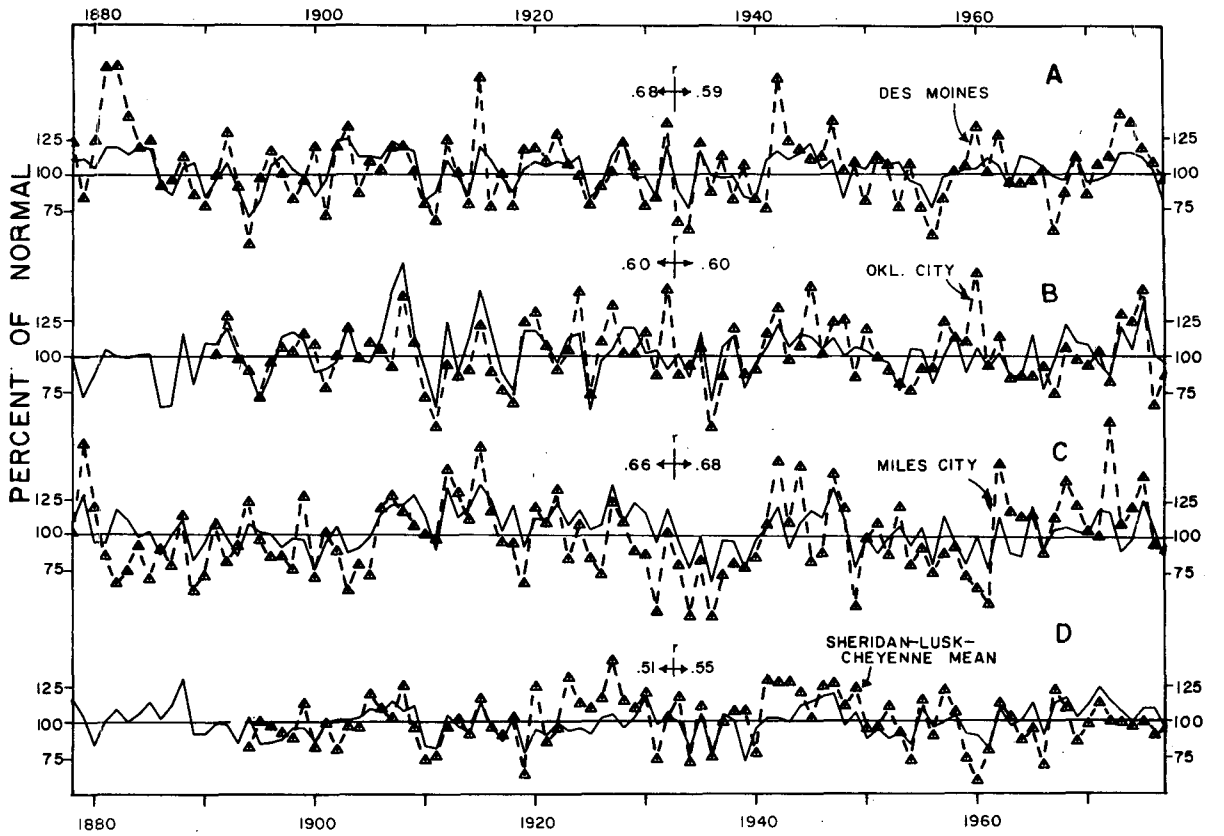

FIG. 4. Time series plots of precipitation series from selected stations (dashed lines) and regional precipitation reconstructions (solid). Series are plotted as percent of 1933–77 normal. Correlation coefficients between actual series and reconstruction are given for both the 1933–77 period and the earlier years.

ring index can be expected to become relatively large as the sample size becomes very small. We evaluated this effect for three of the sites by: 1) recomputing the tree-ring index using only the cores that extended back to the early 1700's; 2) substituting the recomputed indices into the single-site regression equations (Table 2); and 3) comparing the proportion variance explained (R^2 for the period 1933–77) of reconstructions based on the full sample size with R^2 for reconstructions based on the reduced sample size. Values of R^2 are listed below, with respective sample sizes in parentheses:

Arbuckles, OK	0.54 (28)	0.22 (5)
Burning Coal Vein, ND	0.45 (20)	0.47 (10)
Custer, SD	0.45 (38)	0.38 (13)

The calibration period R^2 was clearly misleading for the Arbuckles site, which had the largest change in sample size. The effect at the other two sites was relatively small. Considering sample size changes at other sites, we have restricted subsequent analyses to the post-1700 years in general, and to the post-1750 years for Region B.

5. Discussion of reconstructions

a. Drought history

Prominent in the regional reconstructions is the clustering of drought years and non-drought years (Fig. 3). This feature is clearly seen when the regional reconstructions are summarized in terms of number of regions drier than a specific cutoff level of drought (Fig. 5). Drought years clustered most noticeably in the late 1750's and the 1860's. The persistent recurrence of drought in those periods was unmatched even in the 1930's. Stretches of 10 or more years without drought in any of the regions occurred once or twice per century. The most striking of these periods occurred from 1825 to 1838, immediately after the extreme drought of the early 1820's.

An alternative picture of the large-scale drought history is given by the average of the four regional reconstructions (Fig. 6). The epochs mentioned above are also obvious in the mean series. Long-wavelength fluctuations on the order of greater than 40 years are also vaguely suggested. The sequence of drought-to-wetness-to-drought beginning in the late 1890's and

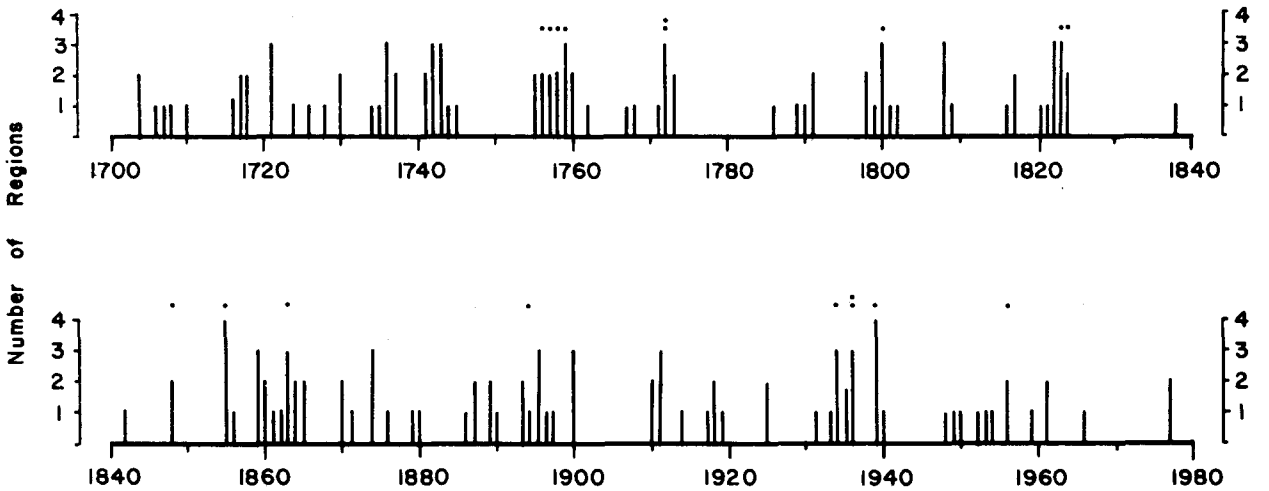

FIG. 5. Number of regions reconstructed in drought for years 1700–1977. Bars indicate number of regions with reconstructed precipitation at least one standard deviation below 1933–77 normal. Dots mark year in which precipitation was at least two standard deviations below normal in one or more regions. Number of dots correspond to number of regions. Standard deviations were computed from 1933–77 reconstructed regional series.

ending about 1940 resembled a similar sequence from the early 1820's to the mid-1860's.

The 1930's were distinguished in the mean reconstruction by the intensity of drought in 1934, 1936 and 1939 (Figs. 5 and 6). When drought conditions were averaged over several years, however, the 1930's drought was milder than the 1750's, 1820's and 1860's. The worst droughts of both the long-term reconstruction and the 1933–77 actual data are listed in Table 4. Note that reconstructions tend to be conservative; reconstructed anomalies were generally smaller than actual anomalies in severe droughts of the 1933–77 period. The years 1936, 1939 and 1934 ranked 3, 4 and 7 in dryness out of 278 years. In terms of three-year moving averages, however, the 1930's were not represented in the top five droughts because of the intercedence of the relatively mild drought year 1935, between two years of extreme drought. For combined intensity and duration, the major historical droughts were centered at approxi-

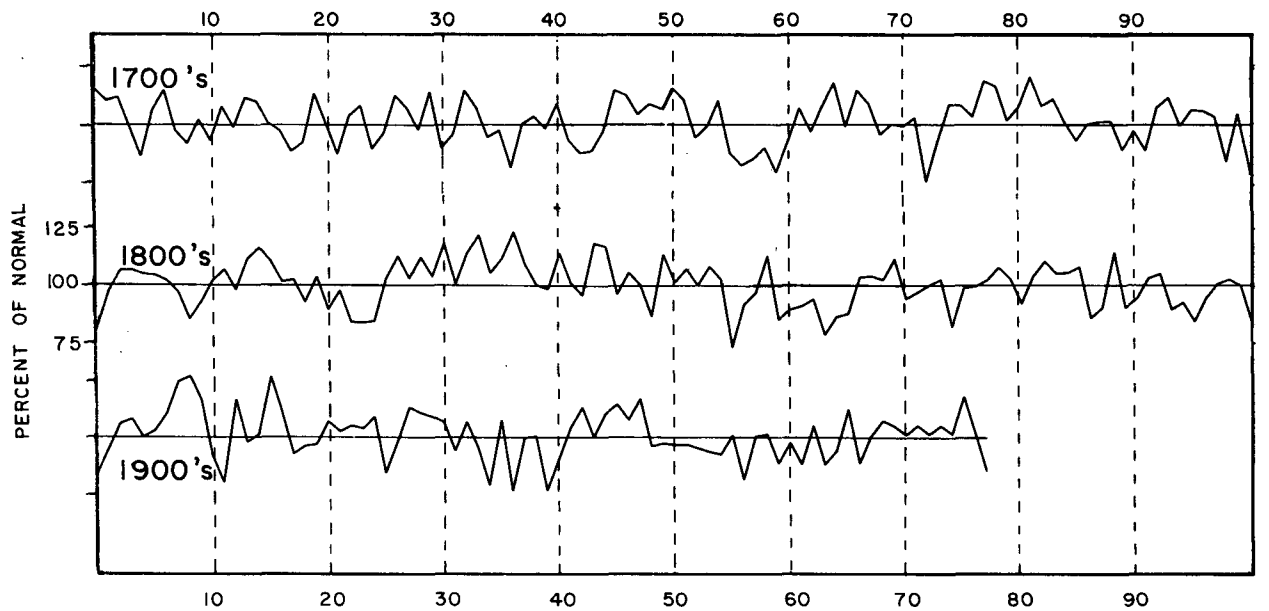

FIG. 6. Time series plot of average of four regional reconstructions. Regional reconstructions were converted to percent of 1933–77 normal before averaging.

TABLE 4. List of driest periods in actual precipitation (1933–77) and in reconstruction (1700–1977). Tabulations were based on mean series formed by 1) converting regional precipitation to percent of 1933–77 normal, and 2) averaging the four regional series.

		Actual		Reconstructed			
		1933–1977		1933–77		1700–1977	
Moving average	Rank[a]	Year[b]	Precipitation[c]	Year	Precipitation	Year	Precipitation
1-year	1	1936	65	1936	78	1855	73
	2	1934	68	1939	78	1772	75
	3	1956	81	1934	80	1936	78
	4	1954	84	1956	83	1939	78
	5	1961	85	1977	87	1863	78
3-year	1	1936	80	1936	89	1824	84
	2	1956	84	1940	90	1865	84
	3	1961	90	1961	93	1759	85
	4	1940	93	1956	93	1857	87
	5	1953	98	1953	96	1861	89
10-year	1	1961	93	1942	95	1864	90
	2	1942	95	1961	95	1761	93
	3	—	(see footnote d)	—		1940	94
	4	—		—		1825	94
	5	—		—		1901	95

[a] Rank of non-overlapping moving averages.
[b] Ending year of moving average.
[c] September–August precipitation expressed as percentage of 1933–77 normal.
[d] Rainfall above normal for all other non-overlapping decades.

mately the following times: late 1750's, early 1820's, early 1860's, mid 1890's, mid 1930's.

The empirical probability of exceeding a given intensity of drought is shown on Fig. 7. The worst drought year of the 1930's had only a 2% chance of being exceeded in a given year; the corresponding probability for the worst drought year of the 1950's was 5%. In terms of 10-year moving averages, the 1930's were exceeded in severity 5% of the time, the 1950's 12% of the time. Extrapolation of probabilities to the future is risky, however, especially considering the evidence of clustering of drought years. Once a "regime" of drought has been entered, drought probability in a given year may be higher than indicated by straightforward empirical probabilities.

6. Spectral properties of reconstructions

Spectral properties of reconstructions were examined with spectral and cross-spectral analysis. The technique employed in this analysis was Fourier transformation of the estimated auto-correlation or cross-correlation function, using the Parzen window and the "window closing" procedure described in Jenkins and Watts (1968). Computations were performed using the Statistical Package for the Social Sciences (SPSS) computer package (Nie *et al.*, 1975). All estimates of statistical significance of sample spectra were made assuming a first-order autoregressive null hypothesis.

a. Frequency response

Periodicity in drought can be inferred from reconstructions only if the reconstructions accurately mir-

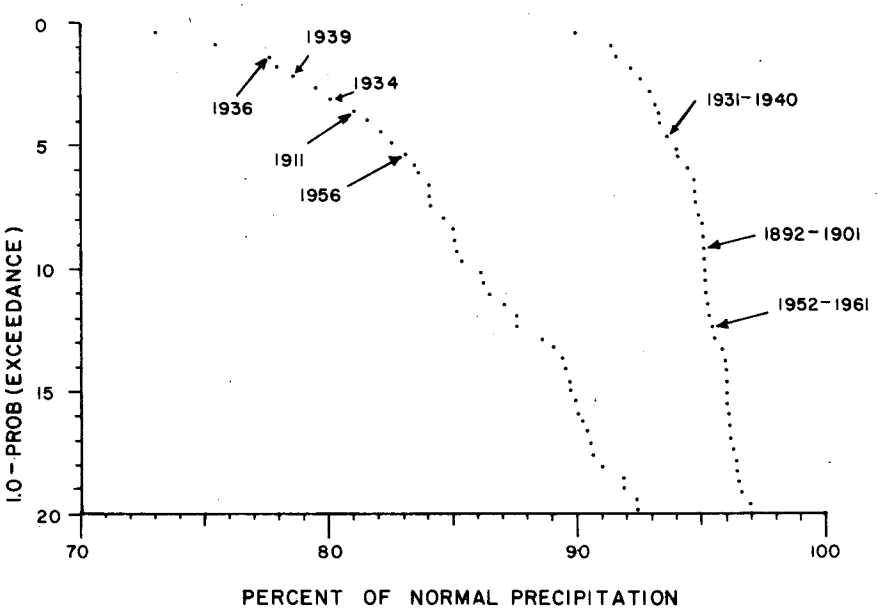

FIG. 7. Empirical probability of drought at various levels of severity. Worst droughts in the present century are noted. Curves were derived from mean series of four regional reconstructions. At left is curve for single years, at right for 10-year moving averages.

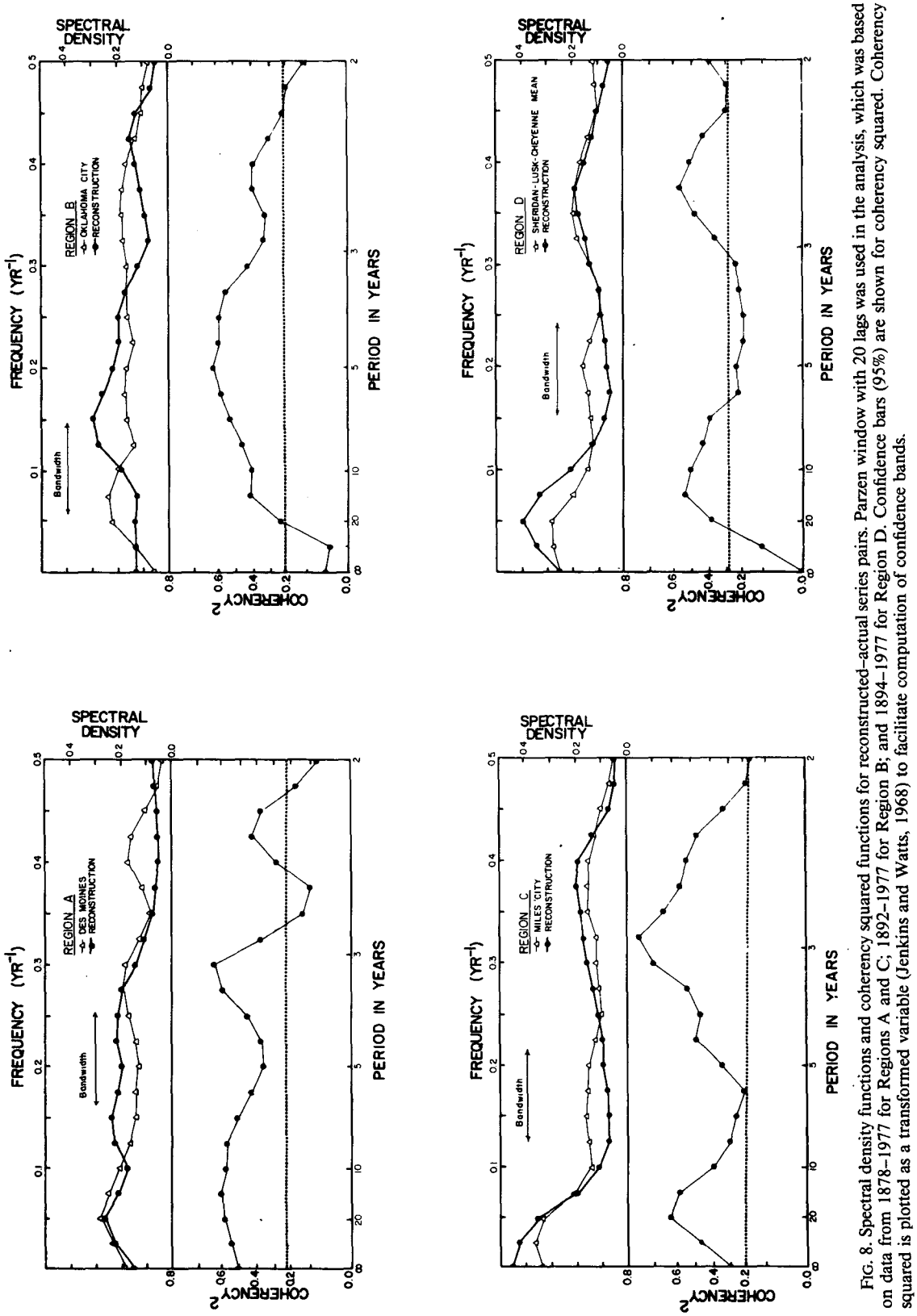

FIG. 8. Spectral density functions and coherency squared functions for reconstructed–actual series pairs. Parzen window with 20 lags was used in the analysis, which was based on data from 1878–1977 for Regions A and C; 1892–1977 for Region B; and 1894–1977 for Region D. Confidence bars (95%) are shown for coherency squared. Coherency squared is plotted as a transformed variable (Jenkins and Watts, 1968) to facilitate computation of confidence bands.

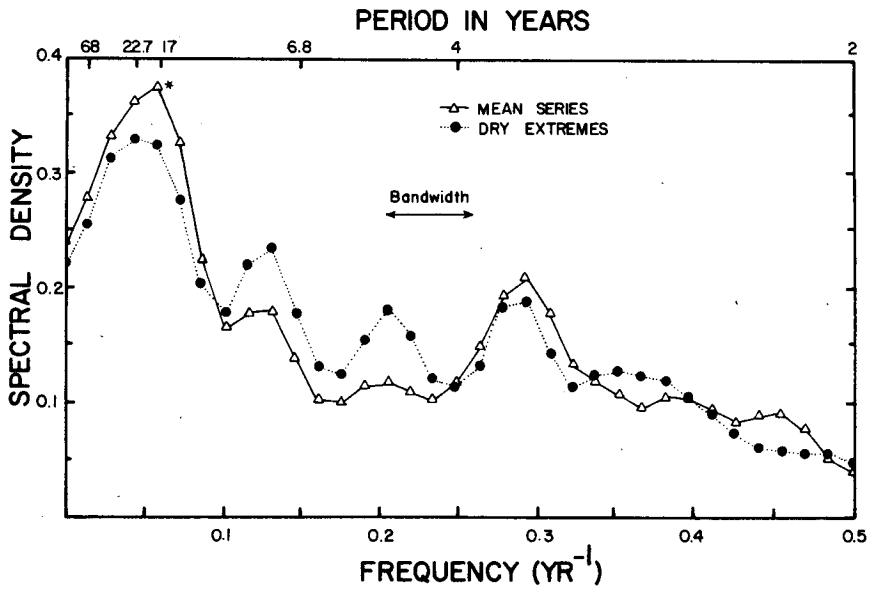

FIG. 9. Spectral density function of mean reconstruction and composite series, 1750–1977 (see text for explanation of series). Star denotes significance at 90% level when tested against first-order autoregressive null hypothesis. Spectral analysis run with Parzen window, 34 lags.

ror the spectral properties of actual precipitation series. Fig. 8 shows, for each region, the estimated spectral density function (SDF) of the regional reconstruction and of an actual precipitation series for a station in the region. Also shown is the coherency-squared plot for each pair. The pairs of series are those whose time series were plotted in Fig. 4; the analysis period ranged from 84 to 100 years in length. With the exception of Region B, major spectral features of actual series are mirrored by similar features in the reconstructions. The reconstruction for Region B had a spectral peak at shorter wavelength than the Oklahoma City series. Consequently, in the particular wavelength of main interest here—22 years—reconstruction B is perhaps the least suitable for searching for periodicity.

The coherency-squared plots, which depict correlation between actual and reconstructed series as a function of frequency, show significant correlation (coherency squared significant at 95% level) for the wavelength band near 20 years in all regions. Note the low coherency squared at very long wavelengths in Regions B and D. Examination of various station precipitation series in Region D revealed large station-to-station differences in long-wavelength fluctuations. The low coherency squared at infinite wavelength for Region D may therefore be strongly dependent on the particular station precipitation series used in the cross-spectral analysis. On the other hand, the low coherency squared at long wavelengths in Region B appears to be due to the relatively weak signal (low variance) in the Oklahoma City series at long wavelengths.

b. Periodicity in long-term reconstructions

The spectral density function of the mean reconstruction, 1750–1977, is shown in Fig. 9. A peak significant at the 90% confidence level is centered at 17 years. Similar analysis of the entire 1700–1977 reconstruction placed the spectral peak at 19 years. This result changed little as the spectral window was varied; the wavelength of the spectral peak ranged from 16 to 19 years.

Also in Fig. 9 is the SDF of a composite series for which the value in any given year is the extreme (driest) of the four regional reconstructions for that year. This series gives a more accurate representation of occurrence of drought "somewhere" in the Great Plains than does the mean series. For example, if the precipitation anomaly in Region A or B were large, but of opposite sign from the anomalies in Regions C and D, then the composite series would show a drought and the mean series would not. The SDF for the composite series peaked at near 22 years, but the peak was not significant at the 90% confidence level.

Spectral density functions of the individual regional reconstructions (Fig. 10) indicated that the main contributors to the peak in the mean series were Regions A and B. In the Iowa region (A), a significant (90%) peak was centered at 23 years; this peak was very stable under window closing, ranging between 22.0 and 23.2 years. In the Oklahoma region (B), a significant (90%) peak was centered at 17 years, with a corresponding range from 16.6 to 22.7 years.

The SDF's of the two westernmost regions (C and D) both had significant (95%) peaks centered near 58

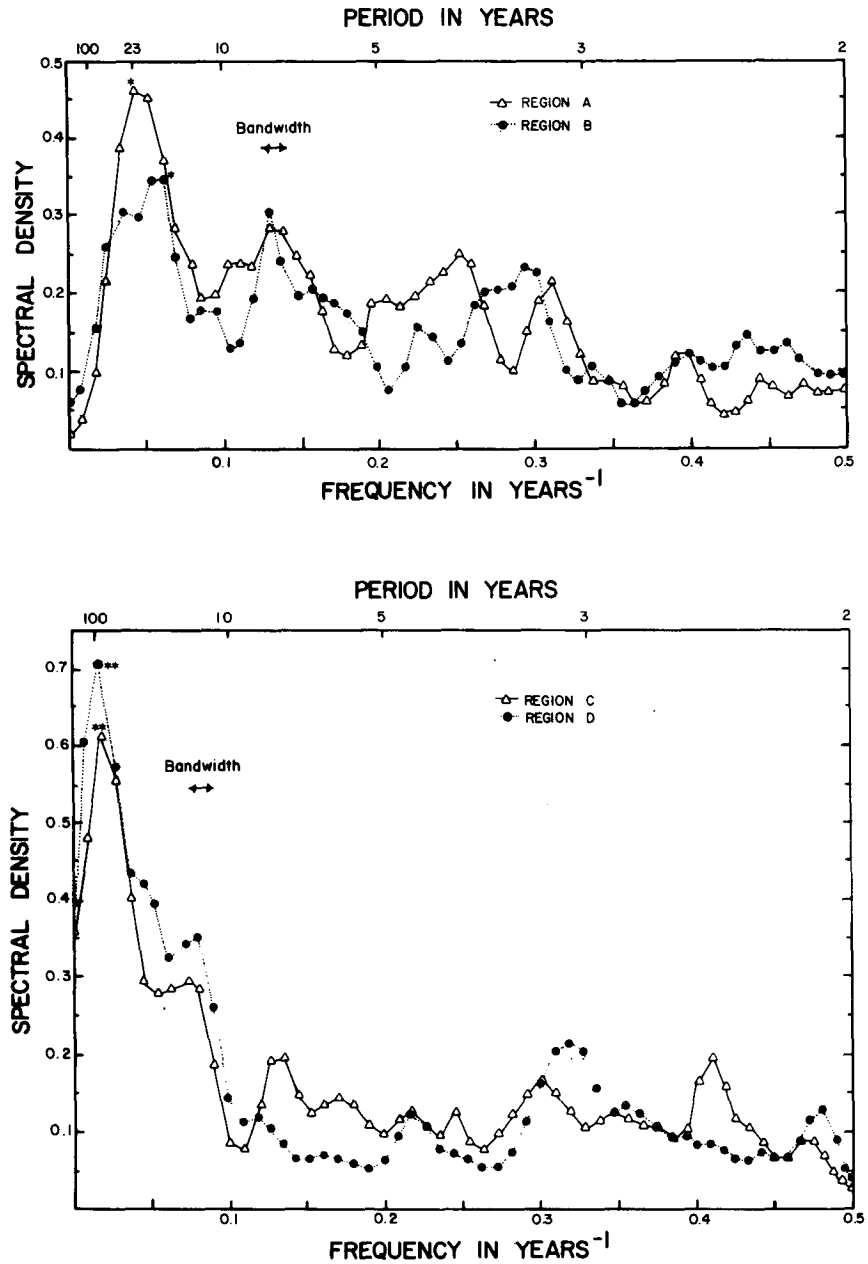

FIG. 10. Spectral density functions of long-term regional reconstructions. One star indicates peak significant at 90% level, two stars at 95% level when tested against first-order autoregressive null hypothesis. Parzen spectral window with 57 lags was used in the analysis. Period analyzed was 1700–1977 for Regions A, C and D; 1750–1977 for Region B.

years. The peak ranged from 58 to 66 years as the lag window was varied. This long-wavelength variation is evident in the time series plots of regional reconstructions (Fig. 3), which also show that the long-wavelength variations in the two regions coincided. This suggests a large-scale influence, since reconstructions for Regions C and D were derived from two completely separate sets of tree ring data.

Spectral analysis of sub-periods of the mean reconstruction indicated that the SDF of the mean reconstruction (Fig. 9) was not equally representative of all parts of the long-term record. SDF's of 88-year sub-periods of the mean reconstruction (Fig. 11) showed a significant (95% confidence level) peak at 14.7 years in 1714–1801, a peak at 22–29 years in the 1890–1977 period, and a peak at 58 years in the middle period, 1802–89. The latter two peaks were not significant at the 90% level.

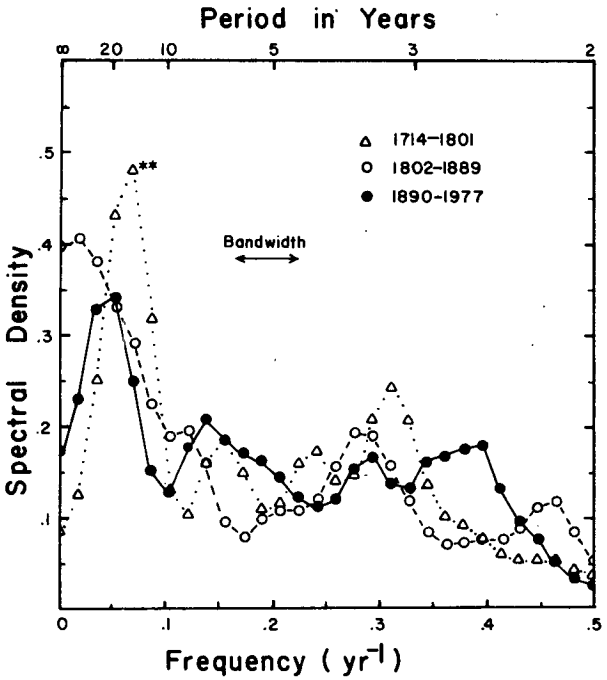

FIG. 11. Spectral density function of mean regional reconstruction estimated for sub-periods of long-term record. The stars denote significance at 95% confidence level when tested against first-order autoregressive null hypothesis. Spectral analysis run with Parzen window, 19 lags.

Sample SDF's for the individual regions by subperiods (not shown) yielded a similar picture, with the exception that in Regions A and B variance was concentrated near 20 years instead of 58 years in the middle period. The sample length for these subperiods (88 years) was of course too short to allow fine resolution of periodicities; the bandwidths shown in Fig. 11 must be considered in discussing particular frequencies of peaks. The following observations were made about a 22-year periodicity in the sub-periods:

1) A spectral peak in the modern (1890–1977) period occurred in three regions; the peak was significant (95%) only in Region D.

2) The periodicity disappeared in the preceding 88 years, except in region B, where it was significant at 90%.

3) A 22-year periodicity was absent from all regions in the 1714–1801 period.

7. Conclusions

The reconstructions indicated that when intensity, duration and regional extent of drought were all considered, the 1930's and 1950's droughts were at least equaled in magnitude by droughts in the following periods: mid-to-late 1750's, early-to-mid 1820's, mid 1850's to late 1860's, and 1890's.

The 1930's, although distinguished by the occurrence of three very dry years, 1934, 1936 and 1939, within a short span of time, were not as severe as the droughts centered about 1860 and 1757 in terms of conditions averaged over three to 10 years. The year 1936 ranked third driest of 278 years, and given the margin of error in the reconstructions, possibly represented the worst single-year drought experienced by the regions as a group. Only 5% of the 10-year periods surveyed were drier than in the 1930's; 12% were drier than the 1950's.

The search for periodicity revealed that drought averaged over the four regions was rhythmic, with an average period near 19 years, but that the periodicity was neither characteristic of all regions, nor of all segments of the drought record in any region. Spectral analysis indicated the following statistically significant (90% or higher significance level) periodicity in the long-term regional reconstructions:

SE Montana	58 years
E Wyoming	58 years
Iowa	22 years
Oklahoma	17 years

The Iowa and Oklahoma regions contributed most to the 19-year periodicity in the mean series. Even in those regions however, the 22-year and 17-year periodicities were not stable over time: separate analyses of 88-year sub-periods showed that from 1714 to 1801, drought in both regions recurred with a 14–15 year period. A near-22-year rhythm in drought showed most clearly in the latest 88 years (1890–1977), less clearly in 1801–89 and not at all in 1714–1801.

These results have several implications for drought prediction. Primarily, assumption of a Great Plains regional 22-year recurrence interval in drought may not be justified, considering the variability in period length; more accurately, drought appears to recur at ill-defined intervals of from 15 to 25 years. Additionally, drought rhythm in one location cannot be generalized to drought rhythm in all locations in the Great Plains. The dominant feature of the drought history in the SE Montana and E Wyoming regions was the long-wavelength variation in precipitation on the order of 58 years; a feature apparently absent from the other two regions. Finally, while these results point out difficulties with drought prediction at specific locations based on a 22-year recurrence period, they do not refute a possible solar–drought connection, especially considering that the solar cycle itself has a variable period length. Apparently, however, whatever effect solar variability may have on drought, it is overwhelmed by other factors at particular locations. The search for a solar–drought connection may be more fruitful if drought recurrence is studied on a considerably larger scale. Additional tree-ring data recently sampled and currently being processed are needed for a more precise picture of large-scale

drought history. We hope to examine this relationship in refined detail in the near future.

Acknowledgments. We thank D. Duvick, T. J. Blasing and D. W. Stahle for use of their tree-ring data from Iowa and Oklahoma. This research was supported by National Science Foundation Grant ATM 7924365.

REFERENCES

Cook, E. R., and G. C. Jacoby, Jr., 1979: Evidence for quasi-periodic July drought in the Hudson Valley, New York. *Nature,* **282,** 390–392.

——, and K. Peters, 1981: The smoothing spline: A new approach to standardizing forest interior tree-ring width series for dendroclimatic studies. *Tree-Ring Bull.,* **41,** 45–53.

Draper, N. R., and H. Smith, 1966: *Applied Regression Analysis.* Wiley, 407 pp.

Duvick, D. N., and T. J. Blasing, 1981: A dendroclimatic reconstruction of annual precipitation amounts in Iowa since 1680. *Water Resour. Res.,* **17,** 1183–1189.

Fritts, H. C., 1962: An approach to dendroclimatology: Screening by means of multiple linear regression techniques. *J. Geophys. Res.,* **67,** 1413–1420.

——, 1976: *Tree Rings and Climate.* Academic Press, 567 pp.

Jenkins, G. M., and D. G. Watts, 1968: *Spectral Analysis and its Applications.* Holden-Day, 525 pp.

Meko, D. M., C. W. Stockton and W. R. Boggess, 1980: A tree-ring reconstruction of drought in southern California. *Water Resour. Bull.,* **16,** 594–600.

Mitchell, J. M., Jr., C. W. Stockton and D. M. Meko, 1979: Evidence of a 22-year rhythm of drought in the western United States related to the Hale solar cycle since the 17th century. *Solar-Terrestrial Influences on Weather and Climate,* B. M. McCormac and T. A. Seliga, Eds., D. Reidel, 125–143.

Nie, N. H., C. H. Hall, J. G. Jenkins, K. Steinbrenner and D. H. Brent, 1975: *Statistical Package for the Social Sciences.* McGraw Hill, 675 pp.

Panofsky, H. A., and G. W. Brier, 1968: *Some Applications of Statistics to Meteorology.* The Pennsylvania State University Press, 224 pp.

Puckett, L. J., 1981: Dendroclimatic estimates of a drought index for northern Virginia. U.S. Water-Supply Pap. 2080, U.S. Govt. Printing Office, 39 pp.

Schulman, E., 1956: *Dendroclimatic Changes in Semiarid America.* University of Arizona Press, 142 pp.

Stockton, C. W., 1975: *Long-term Streamflow Records Reconstructed from Tree Rings.* University of Arizona Press, 111 pp.

——, and D. M. Meko, 1975: A long-term history of drought occurrence in western United States as inferred from tree rings. *Weatherwise,* **28,** 244–249.